Pre-M Phase-promoting Factor Associates with Annulate Lamellae in *Xenopus* Oocytes and Egg Extracts

Clare Beckhelling,*† Patrick Chang,* Sandra Chevalier,* Chris Ford,† and Evelyn Houliston*‡

*Unité Mixte Recherche 7009, Centre National de la Recherche Scientifique/Université Paris VI, Observatoire Oceanologique de Villefranche sur Mer, 06234, Villefranche sur Mer, France; and †School of Biological Sciences, University of Sussex, Falmer, Brighton, BN1 9QG, United Kingdom

We have used complementary biochemical and in vivo approaches to study the compartmentalization of M phase-promoting factor (MPF) in prophase *Xenopus* eggs and oocytes. We first examined the distribution of MPF (Cdc2/CyclinB2) and membranous organelles in high-speed extracts of *Xenopus* eggs made during mitotic prophase. These extracts were found to lack mitochondria, Golgi membranes, and most endoplasmic reticulum (ER) but to contain the bulk of the pre-MPF pool. This pre-MPF could be pelleted by further centrifugation along with components necessary to activate it. On activation, Cdc2/CyclinB2 moved into the soluble fraction. Electron microscopy and Western blot analysis showed that the pre-MPF pellet contained a specific ER subdomain comprising "annulate lamellae" (AL): stacked ER membranes highly enriched in nuclear pores. Colocalization of pre-MPF with AL was demonstrated by anti-CyclinB2 immunofluorescence in prophase oocytes, in which AL are positioned close to the vegetal surface. Green fluorescent protein-CyclinB2 expressed in oocytes also localized at AL. These data suggest that inactive MPF associates with nuclear envelope components just before activation. This association may explain why nuclei and centrosomes stimulate MPF activation and provide a mechanism for targeting of MPF to some of its key substrates.

INTRODUCTION

The structural changes accompanying mitosis and meiosis are governed in almost all species by M phase-promoting factor (MPF) (Masui and Markert, 1971), a complex of Cyclin B and the kinase Cdc2 (reviewed in Nigg, 1995; Morgan, 1997). Direct and indirect targets for MPF include the nuclear envelope and lamina, chromatin proteins, and regulators of mitotic spindle formation (Moreno and Nurse, 1990; Norbury and Nurse, 1992). MPF activation requires the continuous synthesis and accumulation during interphase of Cyclin B, which binds Cdc2 to form inactive pre-MPF. Pre-MPF is maintained inactive by inhibitory phosphorylation on Cdc2 by the Wee1 and Myt1 kinases. At the onset of

mitosis, rapid MPF activation is favored by a positive feedback loop involving Cdc25 phosphatases, MPF itself, and Polo-like kinases. Degradation of Cyclin B at the metaphase-to-anaphase transition by the anaphase promoting complex (APC) destroys the MPF complex and causes exit from mitosis (reviewed in Nurse, 1990; Whitaker and Patel., 1990; Norbury and Nurse, 1992; Nigg, 1995; Morgan, 1997, 1999; Beckhelling and Ford, 1998; O'Farrell, 2001).

Amphibian eggs have proved extremely useful for the study of MPF regulation. Cycles of Cyclin B accumulation and destruction sufficient to drive synchronous cell cycles in the absence of any other protein synthesis occur in both fertilized or activated eggs and in egg extracts (Murray and Kirschner, 1989; Murray *et al.*, 1989; Hartley *et al.*, 1996). Although MPF activation cycles in amphibian oocytes and eggs can continue in the absence of nuclei and microtubules (Hara *et al.*, 1980; Shinagawa, 1983; Gerhart *et al.*, 1984; Newport and Kirschner, 1984; Kimelman *et al.*, 1987; Shinagawa, 1992), two lines of evidence have demonstrated that subcellular structure is important for MPF activation, even in cytoplasmic extracts. First, nuclei, centrosomes and microtubules have all been shown to stimulate MPF activation

Abbreviations used: AL, annulate lamellae; ER, endoplasmic reticulum; HSP, high-speed pellet; HSS, high-speed supernatant; LSS, low-speed supernatant; MPF, M phase-promoting factor.

both in manipulated cells and extracts (Detlaff *et al.*, 1964 and references therein, Gautier, 1987; Iwashita *et al.*, 1998; Pérez-Mongiovi *et al.*, 2000). Second, M-phase entry and exit proceed inhomogeneously within the cell (Masui, 1972; Iwao and Elinson, 1990) and travel as waves from the animal hemisphere, where the nucleus and centrosomes are located, to the vegetal hemisphere (Rankin and Kirschner, 1997; Pérez-Mongiovi *et al.*, 1998). Such observations have led to the suggestion that the nuclear-centrosomal region serves to accumulate MPF and/or its regulators to achieve locally a threshold level that would seed the initial activation of mitosis (Cyert and Kirschner, 1988; Novak and Tyson, 1993; Beckhelling *et al.*, 2000; De Souza *et al.*, 2000). A number of localization studies concerning MPF and its regulators performed in a variety of cell types are consistent with this possibility. B Cyclins, Cdc25, Polo kinase, Wee1, and Myt1 have all been found to localize to structures such as prophase microtubule asters, centrosomes, nuclei, endoplasmic reticulum (ER), and Golgi, their associations with these structures varying with cell cycle time and activity of the molecules involved (Bailly *et al.*, 1989, 1992; Jackman *et al.*, 1995; Liu *et al.*, 1997; Sakamoto *et al.*, 1998; Ashcroft *et al.*, 1999; Ohi and Gould, 1999; Pines, 1999; Charrasse *et al.*, 2000; Takizawa and Morgan, 2000).

Very little is known about the subcellular localization of MPF and its regulators in amphibian eggs. Their large size and yolky cytoplasm severely hampers light microscopy techniques, especially in the deep, nuclear region. We have approached this question by analyzing the distribution of MPF in extracts of prophase eggs fractionated by centrifugation. By prophase, progression through mitosis is completely dependent upon posttranslational changes to the pre-MPF complex because CyclinB has accumulated above the levels required for activation. We focused our analysis on a fraction from prophase *Xenopus* egg extracts previously shown to be necessary for MPF activation (Felix *et al.*, 1989). We found that inactive MPF and inactive Cdc25 were concentrated in this fraction, whereas the active forms of these enzymes were soluble. Electron microscopy (EM) and Western blot analysis unexpectedly revealed that a distinctive ER subpopulation rich in nuclear pores (annulate lamellae, AL), cosedimented with the pre-MPF. This observation led us to explore the localization of pre-MPF with respect to AL in fixed oocytes by immunofluorescence and in live oocytes by CyclinB2-green fluorescent protein (GFP) imaging.

MATERIALS AND METHODS

Antibodies and Reagents

Primary antibodies were as follows: anti-PSTAIR monoclonal antibody (mAb) (Sigma-Aldrich, St. Louis, MO); affinity purified anti-*Xenopus* CyclinB2 antibody from rabbit serum (provided by M. Dorée, Center de Recherches de Biochimie Macromoleculaire, Montpellier, France); rabbit anti-*Xenopus* Cdc25C polyclonal antibody (provided by E. Shibuya, University of Alberta, Edmonton, Canada); anti-GRP94 rat mAb (StressGen Biotechnologies, Victoria, British Columbia, Canada) used as an ER marker (Argon and Simen, 1999; Brunati *et al.*, 2000); and anti-human mitochondrial voltage dependent anion channel (VDAC) polyclonal rabbit antibody raised against CSPNTGKKNAKIKTGYKREH (provided by M. Colombini, Department of Biology, University of Maryland, College Park, MD) used as a mitochondrial marker. Nuclear pore proteins were detected with anti-Nup mAb, QE5 (Eurogentec, Seriang, Belgium),

and anti-γ-tubulin with mAb GTU-88 (Sigma-Aldrich). Golgi markers were anti-syntaxin and GS15 (BD Biosciences, Erembodegem, Belgium). 1,2-Bis(2-aminophenoxy)ethane-*N*,*N*,*N'*,*N'*-tetraacetic acid (BAPTA) (Calbiochem, San Diego, CA) was dissolved at 250 mM in water and neutralized to pH 7.0 with concentrated HCl. Cytochalasin B was stored as a stock solution of 10 mg/ml in dimethyl sulfoxide (DMSO). Stocks of aprotinin and leupeptin were stored at 10 mg/ml in water, pepstatin at 5 mg/ml in DMSO, and 4-(2-aminoethyl)benzenesulfonyl fluoride at 0.2 M in water. All other reagents were from Sigma-Aldrich unless otherwise stated.

Extracts and Centrifugation

Female *Xenopus laevis* (Center National de la Recherche Scientifique Rennes, France; Horst Kähler, Hamburg, Germany; or Blades Biological, Cowden, England), preinjected in some experiments with 50 IU of pregnant mare serum, were induced to ovulate by injection of ~750 IU of human chorionic gonadotropin (Organon Teknika, West Chester, PA). Eggs were laid into high salt water (110 mM NaCl in stored tap water at 21°C). The jelly coat was removed using a solution containing 110 mM NaCl, 20 mM Tris pH 8.5, 5 mM dithiothreitol (DTT). Eggs were then washed gently three times in Barth X [110 mM NaCl, 10 mM HEPES, 2.4 mM NaHCO$_3$, 1 mM KCl, 0.8 mM MgSO$_4$, 0.4 mM CaCl$_2$, 0.33 mM Ca(NO$_3$)$_2$, pH 7.6]. Necrotic or activated eggs were removed.

Preparation and fractionation of extracts were based on a protocol devised by Felix *et al.*, (1989) with the modifications of Lindsay *et al.* (1995). The protocol is summarized in Figure 1. Eggs were activated in glass dishes with ionophore A23187 at a final concentration of 0.1 µg/ml. Ionophore was diluted from a stock solution of 1 mg/ml (in DMSO) into 50 ml of 25% (vol/vol) Barth X. Eggs were left in ionophore solution for 2 min and then washed with two changes of 25% (vol/vol) Barth X. Activated eggs from two to four females (5–15 ml of eggs) were incubated at 21°C for 55–60 min and then transferred to a 50-ml tube and washed twice in ice cold extraction buffer (EB, 100 mM K-acetate, 2.5 mM Mg-acetate, 1 mM DTT, 20 mM HEPES pH 7.2, 250 mM sucrose). Eggs were transferred to a minimal volume of ice cold extraction buffer containing 2.5 mM 1,2-bis(2-aminophenoxy)ethane-*N*,*N*,*N'*,*N'*-tetraacetic acid, 5 µg/ml cytochalasin B, and protease inhibitors (10 µg/ml aprotinin, 10 µg/ml leupeptin, 0.76 mM 4-(2-aminoethyl)benzenesulfonyl fluoride, 15 µg/ml pepstatin) in 5-ml plastic centrifuge tubes and packed by centrifugation at 700 rpm in a Jouan CR 4-11 centrifuge. Excess buffer was removed. The eggs were then centrifuged at 12,000 rpm (~10,000 × g) for 12 min at 4°C in a Beckman Coulter L8-55 M ultracentrifuge (rotor SW55). The low-speed supernatant (LSS) between the lipid cap and the pigment/yolk pellet was removed with a cold Pasteur pipette or by side puncturing the tube with a syringe and wide bore needle. The LSS was centrifuged at 48,000 rpm (245,000 × g) for 2 h at 4°C in 5-ml tubes if sufficient volume, otherwise in 0.6-ml tubes with adapters in the SW55 rotor. The resultant high-speed supernatant (HSS) was removed by side puncture of the tube with a syringe and wide gauge needle. At least three distinct layers of high-speed pellet were distinguishable: a dense orange pellet, presumed to be glycogen (Meier *et al.*, 1995) overlain successively by a dark brown pellet (HSP-1a) and a yellow layer (HSP-1b). HSP-1a and -1b were removed with wide-mouthed pipette tips and swirled into EB containing protease inhibitors in 5-ml centrifuge tubes. These were then recentrifuged at 20,000 rpm for 20 min at 4°C in the SW55 rotor. After this washing step, each pellet was combined with an equal volume of 60% (wt/vol) sucrose (in EB containing protease inhibitors) and snap frozen in 5-µl aliquots in liquid nitrogen. Aliquots (50 µl) of HSS were also snap frozen.

To fractionate the HSS-1 further, it was mixed with an equal volume of ice-cold extraction buffer containing protease inhibitors and "energy mix" (1 µl/50 µl of extract): 500 mM creatine phosphate, 4 mg/ml creatine phosphokinase (in 50% glycerol [vol/vol] in H$_2$O), and 50 mM ATP (pH 7.0 in 20 mM HEPES). After mixing, 2 ml of diluted supernatant were transferred to 3-ml thick-walled polycarbonate tubes and
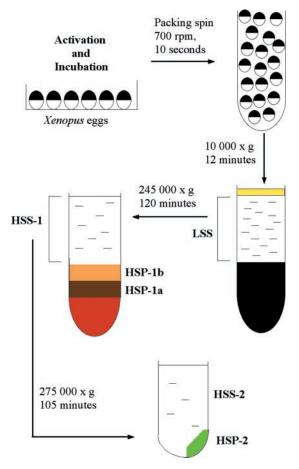
Figure 1. Preparation of high-speed fractions of egg extracts. Eggs, taken 60 min after activation, were subject to a brief packing spin before low-speed centrifugation to crush them, separating supernatant (LSS) from yolk pellet and lipid layer. High-speed centrifugation stratified supernatant (HSS-1) from differently colored pellet fractions (HSP-1a, HSP-1b) above a gelatinous orange layer that was discarded. Dilution and further centrifugation of HSS-1 generated HSS-2 and HSP-2. See MATERIALS AND METHODS for detailed explanation.

centrifuged at 68,000 rpm (275,000 × g) at 4°C for 1 h 45 min in a fixed angle rotor (TLA100.3) in a TL100 tabletop centrifuge. The resultant ultrahigh-speed supernatant (HSS-2) and an ultrahigh-speed pellet (HSP-2) were separated by removing the supernatant with a Pasteur pipette. HSP-2 consisted of a lighter "fluffy" part and a viscous part. The supernatant was removed carefully by pipetting up to the "fluffy" part of the pellet. This routinely left ~100 μl of supernatant and pellet, which were then mixed to resuspend both parts of the pellet with a wide-mouthed pipette tip. HSP-2 was diluted 1:1 with 60% (wt/vol) sucrose (in EB containing protease inhibitors) before snap freezing as 5-μl aliquots in liquid nitrogen. HSS-2 was snap frozen as 10- or 100-μl aliquots. Average protein concentrations of the fractions were determined by standard Bradford assay (Bio-Rad, Hercules, CA) and were as follows: 30–40 mg/ml HSS-1, 40–50 mg/ml HSP-1a, 40–50 mg/ml HSP-1b, 10–25 mg/ml HSS-2, and 40–50 mg/ml HSP-2.

SDS-PAGE and Western Blotting

Each extract fraction was combined on thawing with 1 volume of water and 6 volumes of 2× SDS sample buffer (Laemmli, 1970)

except HSS-2, which was combined with 3 volumes of 2× SDS sample buffer. Samples were boiled for 4 min before loading 20 μg of protein onto SDS-polyacrylamide gels: 8% for Nup, 10% for Cdc25/CyclinB2/PSTAIRE, and 12% for GRP94/VDAC. Electrophoresis was performed for 3–4 h at 100 V with a maximum of 250 mA in running buffer (0.1% SDS, 0.025 M Tris, 0.192 M glycine; Laemmli, 1970).

Transfers onto nitrocellulose paper (Shleicher & Schuell, Keene, NH) were carried out in 0.025 M Tris/0.192 M glycine/15% methanol at 100 V for 60 min. For immunodetection, the protocol was exactly as in Pérez-Mongiovi et al., (2000). Primary antibodies were Cdc25, 1/2000; CyclinB2, 1:500; PSTAIRE, 1:2000; GRP94, 1:2000; VDAC, 1:2000; and Nup, 1:500.

Electron Microscopy

Samples (not >50 μl) for thin sectioning were diluted ~50-fold into phosphate-buffered saline (PBS) containing 0.1 M sucrose, 2% glutaraldehyde, and 2% osmium tetroxide for 30 min on ice, before pelleting at 4000 rpm in a Jouan CR 4-11 centrifuge at 4°C for 10 min. The pellets were washed in PBS/sucrose before dehydration in a graded series of ethanol (50, 60, 70, 80, 90, 95, and 3 × 100%). The pellets were embedded in Spurr's resin and baked at 70°C overnight. Silver sections cut from the blocks were poststained on grids with 2% uranyl acetate followed by lead citrate. Micrographs were taken with a Hitachi H-600 electron microscope. Negative staining was carried out according to the protocol of Meier et al. (1995) with modifications. A 10-μl sample of unfixed HSP-2 was washed in 50 μl of ice-cold wash buffer (10 mM HEPES pH 7.4, 3 mM MgCl$_2$ containing protease inhibitors as for EB; see above) in a 1.5-ml Eppendorf tube and centrifuged in a benchtop centrifuge at 4°C for 5 min at 14,000 rpm. The pelleted material (4 μl) was deposited onto a glow discharged pioloform-coated grid washed briefly with H$_2$O and then placed face down into a drop of 2% uranyl acetate for ~1 min, blotted dry, and immediately observed in the electron microscope as described above.

Histone Kinase Assays

HSS-1 was rapidly thawed and supplemented with energy mix as described above. For HSS-2 and HSP-2, no further energy was added. HSP-2 was pipetted with a wide-mouthed pipette tip and generally 3 μl of HSP-2 was combined with either 27 μl of HSS-2 or extraction buffer (containing energy as described above) for incubation purposes. Aliquots (30 μl) of extracts were transferred to 21°C and 2 μl was removed every 10 min, diluted 1/25 in ice-cold histone kinase buffer (80 mM β-glycerophosphate, 20 mM EGTA, 15 mM MgCl$_2$, 1 mM DTT pH 7.3, 10 μg/ml aprotinin, 10 μg/ml leupeptin), and frozen in liquid nitrogen before storing at −80°C. Histone (H1) kinase assays were carried out as described previously (Beckhelling et al., 1999).

Immunofluorescence and Confocal Microscopy

Oocytes were fixed at −20°C in methanol containing 1% formaldehyde for a minimum of 2 h. After stepwise rehydration to PBS containing 0.05% Triton X-100 at room temperature, oocytes were extracted for 15 min in PBS/0.25% Triton X-100, rinsed in PBS, and blocked for 1 h in 2% bovine serum albumin/PBS. Oocytes were incubated in 50 μl of the following primary antibodies: rat mAb GRP94 at 1/500; mouse mAb NUP at 1/500; and rabbit polyclonal antibody CyclinB2 at 1/50 overnight at 4°C to detect ER, AL, and associated molecules. Oocytes were washed at least three times in PBS/0.1% Tween 20 before incubation in either rhodamine (at 1/75) and/or fluorescein isothiocyanate-labeled (at 1/100) secondary antibodies (Jackson Immunoresearch Laboratories, West Grove, PA) at room temperature for 2 h and mounted in Citifluor (Department of Chemistry, University of Kent, Kent, United Kingdom) after repeating the washing step. Confocal images were acquired on an inverted
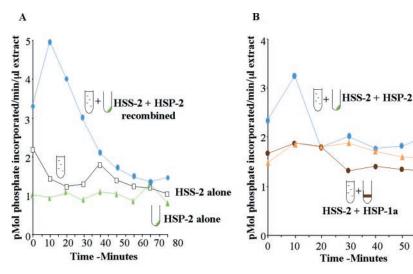
Figure 2. Histone (H1) kinase activity of fractions incubated separately and in combination. Samples of each fraction were either diluted into extraction buffer or combined with HSS-2 before transfer to 21°C. Aliquots were taken every 10 min for up to 80 min for assay of histone (H1) kinase activity, expressed as picomoles of phosphate transferred per minute per microliter of extract. (A) HSS-2 alone (open squares), HSP-2 alone (green triangles), and HSS-2 recombined with HSP-2 (blue circles). Neither fraction can activate H1 kinase alone but when recombined stimulate one cycle of activation and inactivation of H1 kinase. (B) From a different extract, HSS-2 was recombined with either HSP-2 (blue circles), HSP-1a (brown circles), or HSP-1b (yellow triangles). Only HSP-2 stimulated one cycle of mitotic histone (H1) kinase activation and inactivation when combined with HSS-2.

Leica SP2 confocal microscope equipped with Argon and Green neon lasers and associated software and subsequently processed using NIH Image software. Controls in which primary antibodies were omitted confirmed that no cross-reaction between antibodies occurred.

Synthesis and Microinjection of GFP and GFP-CyclinB2 RNA

Xenopus CyclinB2 was obtained from M. Dorée and inserted into plasmid CS2-GFP (such that the GFP sequence was at the C terminal of CyclinB2) containing the S65T variant of GFP with linker sequence AHRL (Heim *et al.*, 1995). A nonconjugated GFP mRNA was transcribed from the RN3-GFP plasmid (Zernicka-Goetz *et al.*, 1996). mRNA coding for the GFP or GFP-CyclinB2 constructs were made using mMessage mMachine kit (Ambion, Austin, TX), purified in a ProbeQuant kit (Amersham Biosciences, Piscataway, NJ) and stored in diethyl pyrocarbonate-treated H_2O at -80°C.

Pieces of *Xenopus* ovary were rotary shaken in collagenase B (1 mg/ml) in Na_2HPO_4 (100 mM), pH 7.4, for 30 min before transferring to OR2 (2.5 mM KCl, 82 mM NaCl, 50 mM HEPES, 10 mM Na_2HPO_4, 1 mM $CaCl_2$, 1 mM $MgCl_2$) for manual defolliculation of the stage VI oocytes (Dumont, 1972). Oocytes were cultured overnight in 50% Leibowitz solution containing penicillin (10 U/ml), streptamycin (0.01 mg/ml), gentamicin (0.1 mg/ml), and bovine serum albumin (1 mg/ml; Euromedex, Souffelweyersheim, France) and then were injected with ~16 nl of RNA by using a Drummond Nanoject to deliver a final amount of ~4.2 ng of CyclinB2-GFP mRNA or 5.3 ng of GFP mRNA. Oocytes were mounted in chambers consisting of a glass slide and coverslip separated by a silicone rubber spacer at various times after injection for observation of fluorescence beneath the vegetal surface by using the confocal microscope as described above.

RESULTS

A Fraction Pelleted from High-Speed Supernatants Is Necessary for MPF Activation

HSS of *Xenopus* eggs made at prophase spontaneously undergo one cycle of MPF activation and inactivation (measured by histone H1 kinase activity), when incubated at 21°C. Dilution and recentrifugation of the HSS produce a particulate fraction that is absolutely required for MPF activation (Felix *et al.*, 1989). We have analyzed the structural composition and partitioning of MPF in fractions prepared by an equivalent protocol (Figure 1). High-speed centrifugation of crushed egg supernatant (LSS; Figure 1), prepared 60 min after egg activation, produced dark brown (HSP-1a) and yellow (HSP-1b) pellet fractions and supernatant (HSS-1) that, on dilution and further centrifugation, generated a final supernatant (HSS-2) and the second high-speed pellet (HSP-2) necessary for MPF activation.

Most HSS-1 preparations prepared 60 min after activation displayed a cycle of MPF activation and inactivation (monitored as histone H1 kinase activity). All of these could be fractionated into HSS-2 and HSP-2 that alone were insufficient for MPF activity but when recombined mirrored H1 kinase activity of the HSS-1 (Figure 2A; Felix *et al.*, 1989), albeit with a lower total level of activity due to the twofold dilution. In contrast, the HSP-1a and HSP-1b pellets could not substitute for HSP-2 to promote H1 kinase activity when combined with HSS-2 in most experiments (Figure 2B). In some extracts, these pellets did permit a rise in MPF activity when combined with HSS-2 but never to the same high levels as those of the HSP-2/HSS-2 combination. Given the different ability of these fractions to support MPF activation, we went on to compare their composition first in terms of membranous organelles and second of MPF regulatory molecules.

HSP-2 Is Enriched in Nuclear Pore Proteins and Annulate Lammellae

Western blots using antibodies recognizing different intracellular compartments (Figure 3, A–D) in parallel with transmission electron microscopy (TEM) analysis (Figure 4, A–D) revealed a distinct separation of organelles between each of the pelleted fractions. The HSP-1a was found to contain the bulk of the mitochondria. The mitochondrial VDAC (Xu *et*
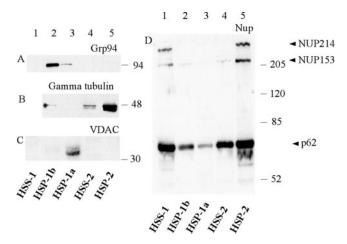
Figure 3. Enrichment of nuclear pore proteins in HSP-2. Twenty micrograms (as determined by Bradford assay) of each fraction obtained by serial centrifugation of prophase extracts (Figure 1) was loaded onto different percentages of gels depending upon the antibody to be used, transferred to nitrocellulose, and probed with the antibodies indicated. HSP-1b was highly enriched in ER protein, GRP94 (A, lane 2), whereas HSP-1a was enriched in the mitochondrial protein VDAC (C, lane 3). HSP-2 contained three nuclear pore proteins detected by the anti-NUP antibody: NUP214, NUP153, and p62 (arrowheads in D, lane 5). HSP-2 was also enriched in γ-tubulin (B, lane 5). In all immunoblots, lane 1 contains an unfractionated HSS-1 and lane 4 contains the HSS-2 made by dilution and recentrifugation of HSS-1.

al., 1999) was detected exclusively in this fraction (Figure 3C, lane 3). TEM analysis of fixed and sectioned pellets confirmed that HSP-1a contained high concentrations of mitochondria with some ribosomal-sized particles (Figure 4A). The HSP-1b contained the bulk of the ER luminal protein GRP94 (Argon and Simen, 1999) (Figure 3A, lane 2) and contained filamentous strands associated with numerous ribosomal-sized particles consistent with the characteristics of rough ER (Figure 4B). Two Golgi markers (syntaxin and GS15) distributed approximately equally between the HSP-1a and HSP-1b but were absent from other fractions (our unpublished data).

HSP-2, the fraction necessary for MPF activation, was found by TEM to contain abundant granular material as well as stacks of membranes (Figure 4C). These stacks consisted of double membranes interrupted by regular breaks characteristic of AL, a specialized region of the ER containing a high density of nuclear pore complexes. Pores were observed as holes at regular intervals crossing the membranes in regions where membrane stacks were sectioned transversely and as annuli when sectioned tangentially. The presence of pore complexes in the HSP-2 in a second extract was confirmed by negative staining (Figure 4D). The observed ring structures were ~90 nm in diameter, falling within the 85- to 120-nm range reported for pore complexes (Kessel, 1992). The presence of nuclear membrane components in HSP-2 was confirmed by Western blotting with a mAb generated against rat liver nuclear envelope proteins (Pante et al., 1994) (Figure 3D, lane 5). This antibody recognizes at least three major nuclear pore proteins: NUP214 located on the cytoplasmic filaments of the nuclear pore complex;

NUP153 situated on the terminal ring of the nucleoplasmic basket; and, p62, which localizes to the inner ring of the pore (Pante et al., 1994). All three NUP proteins were strikingly enriched in HSP-2 (Figure 3D, lane 5), although p62 was found in variable amounts in all fractions (compare lanes 1–4). The HSP-2 was also enriched in γ-tubulin (Figure 3B).

Taken together, the immunodetection and EM results indicate that the first high-speed centrifugation pellets the majority of the mitochondria, Golgi, and ER from the extracts, while stratifying them into HSP-1a and HSP-1b, respectively. A subfraction of the ER enriched in nuclear envelope components is retained in the first HSS but is then pelleted by the second high-speed centrifugation after dilution. Granular material that may contain proteinaceous complexes, including γ-tubulin ring complexes, is also pelleted upon further dilution and centrifugation.

Compartmentalisation of Active and Inactive Cdc25C and MPF

We examined the distribution of MPF regulatory molecules in the various extract fractions on Western blots in three different ways. First, we analyzed the distribution of these molecules and their different isoforms in an unfractionated LSS and among the separated fractions (Figure 5A). We then followed a time course of the behavior of Cdc25C and CyclinB2 in aliquots of HSS-2 and HSP-2 incubated at 21°C separately and recombined (Figure 5B). Finally, we compared the partitioning of activating isoforms of Cdc25C and CyclinB2 between the HSS-2 and HSP-2 in different extracts, which were prepared at slightly different times during the MPF activation process (Figure 5C). Figure 5A shows an experiment in which equal amounts of protein from each fraction were loaded onto gels and immunoblotted by using antibodies that recognize Cdc25C, CyclinB2, and Cdc2 (PSTAIR antibody). A striking compartmentalization of active and inactive forms of MPF and Cdc25C was observed between the high-speed fractions, recognizable as changes in electrophoretic mobility caused by the different regulatory phosphorylations. Cdc25C is hyperphosphorylated when active and migrates distinctly higher on gels than the unphosphorylated inactive form. In contrast, the phosphorylated (upper) isoforms of Cdc2 are inactive and dephosphorylation leading to activation causes a shift to a lower band. Abundant monomeric inactive Cdc2 also migrates in the lower band (Edgar et al., 1994; Pérez-Mongiovi et al., 2000). Because our extracts were made at a time corresponding to the beginning of mitosis, most CyclinB is nonphosphorylated and present in the inactive pre-MPF complex, containing inactive phosphorylated Cdc2. CyclinB is intraphosphorylated by activated Cdc2/CyclinB (Borgne et al., 1999) and the appearance of the upper form of CyclinB2 has been shown to strictly correlate with GVBD/metaphase in maturing Xenopus oocytes (Kobayashi et al., 1991). The appearance of the phosphorylated (upper) form can be considered to be a marker of MPF activation.

After initial centrifugation of the LSS (lane 1) most Cdc25C, CyclinB2, and Cdc2 remained in the first high-speed supernatant (HSS-1, lanes 2 and 3). In comparison, relatively little Cdc2/CyclinB or Cdc25C was found associated with either ER- (HSP-1B, lane 4) or mitochondrial (HSP-1a, lane 5)-enriched pellets, although the mitochondrial fraction seemed to contain some distinct Cdc25 isoforms.
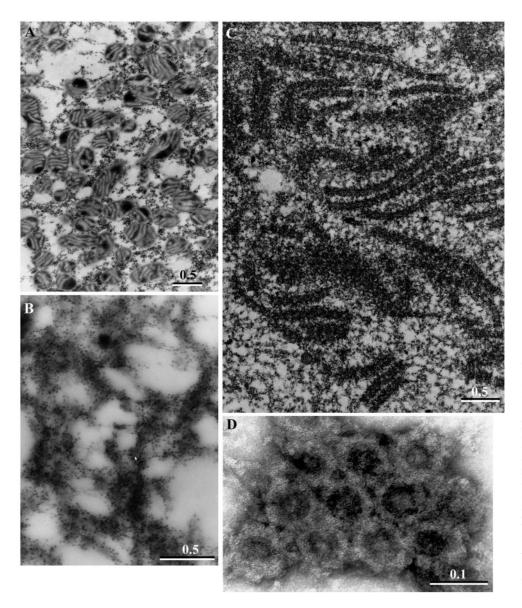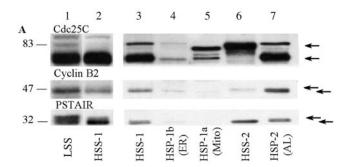
Figure 4. Annulate lamellae are enriched in HSP-2. TEM and negative staining were used to identify structures in the pelleted fractions. (A) Image of HSP-1a, showing mitochondria and some putative ribosomal material. (B) Image of HSP-1b, membranes covered in ribosome-sized particles consistent with an enrichment of ER. (C) Image of HSP-2, containing granular material and stacks of membranes containing identifiable nuclear pore complexes. The membranes have been sectioned both transversely and tangentially. Pore complexes were also detected by negative staining in HSP-2 from another extract (D). Bars, 0.5 μm in A–C and 0.1 μm in D.

Two important observations were made after fractionation of HSS-1. First, the majority of the CyclinB2, along with inactive isoforms of Cdc25C and the inactive (phosphorylated upper) form of Cdc2 pelleted in the HSP-2 (lane7). The presence of all the detectable inhibitorily phosphorylated Cdc2 in this pellet infers that the majority of pre-MPF, consisting of inactive Cdc2 bound to both major egg B cyclins (B1 and B2), sediments in this fraction. Second, the HSS-2 (lane 6) contained the activated isoforms of Cdc25C, along with Cdc2 as active and/or nonphosphorylated isoforms, and variable amounts of phosphorylated CyclinB2, indicative of active MPF. These observations indicate that although the majority of the inactive pre-MPF present at the time these extracts were made was in a pelletable form, active MPF was present in both the soluble (HSS-2) and insoluble (HSP-2) fractions.

Figure 5B shows a time course of the phosphorylation status of CyclinB2 and Cdc25C followed in HSS-2 and HSP-2 separately and in HSS-2/HSP-2 recombined upon incubation at 21°C from 0 to 30 min. In recombined aliquots of HSS-2/HSP-2 (Figure 5B, top), a full cycle of MPF activation and inactivation occurred with phosphorylation of Cdc25C reaching a peak at 20 min, before undergoing dephosphorylation. The doublet band of Cyclin B2 shifted to favor the upper phosphorylated form by 10 min and had degraded by 20 min. In contrast, in HSS-2 incubated alone (middle), Cdc25C activated within 5 min of transfer to 21°C but failed to inactivate, whereas the small amount of Cyclin B2 (present mainly as the activated upper isoform) remained stable. In the HSP-2 (bottom), the Cdc25C was unable to activate in the absence of the supernatant and CyclinB2 failed to degrade. These data indicate that the pelletable
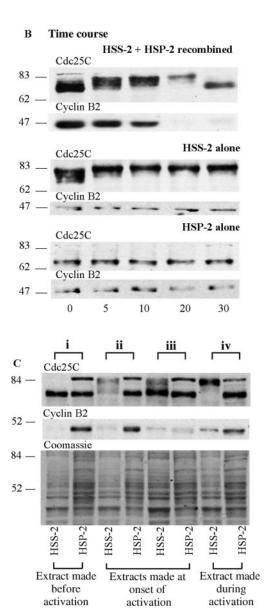
Figure 5. (A) Pre-MPF and inactive Cdc25C preferentially pellet into HSP-2. Immunoblots showing the different isoforms of MPF and Cdc25C in prophase LSS and HSS-1 run on the same gel (lanes 1 and 2) and in the various high-speed fractions run on a second gel

populations of Cdc25C and pre-MPF cannot activate in the absence of a soluble component. In contrast, part of the MPF activation-inactivation loop involving Cdc25C can occur in the aqueous compartment of the egg, but without the pellet components in the HSP-2 it cannot complete. Part of an explanation for these observations may be that an inhibitor of Cdc25C is present in the pellet, thus preventing activation in this fraction.

MPF Shifts from the HSP-2 to the Supernatant upon Activation

Comparison of CyclinB2 and Cdc25C distribution in extracts prepared at slightly different times with respect to the advancement of the cell cycle allowed us to demonstrate that MPF shifts from the pellet to the supernatant in parallel with activation. The HSS-2 and HSP-2 from four different extracts (Figure 5C, i–iv) were migrated in parallel and immunoblotted for Cdc25C and CyclinB2. The time taken for these different extracts to undergo MPF activation at 21°C was

(lanes 3–7, equal loading was confirmed by Coomassie blue staining, our unpublished data). After electrophoretic transfer, different molecular weight regions of the same blot were probed with the antibodies indicated above each horizontal strip. Most of the CyclinB2 and Cdc2 present in the initial LSS extract remained in the supernatant (HSS-1) after high-speed centrifugation. The second high-speed centrifugation pelleted most inactive Cdc25C (lower arrow, hypophosphorylated form) and inactive, phosphorylated Cdc2 (upper arrow in PSTAIR blot), together with most of the CyclinB2, representing the pre-MPF predominant in these extracts (lane 7). In contrast, the small amount of active MPF present in the original prophase extracts was retained in the final soluble fraction (HSS-2, lane 6), as indicated by the presence of CyclinB2 predominantly in the phosphorylated form (upper arrow) associated with activating/activated MPF and the absence of the inactive Cdc2 isoforms. Multiply phosphorylated Cdc25C (upper arrow) was also present in the HSS-2. (B) Cdc25C can activate in the supernatant alone but not in the pellet alone. Volumes (30 μl) of either recombined HSS-2 + HSP-2 or HSS-2 alone or HSP-2 alone were transferred to 21°C and aliquots were taken every 5–10 min for 30 min (indicated at the bottom of the figure). A typical time course of activation (phosphorylation and shift to the upper isoforms) and inactivation (dephosphorylation and down shift on the gel) of Cdc25C occurred >30 min in the recombined aliquots (top). Activation without inactivation was observed in the HSS-2 alone, whereas no activation occurred in the HSP-2 alone. Approximate relative molecular weights in kilodaltons are shown on the left. (C) Activated forms of CyclinB2 shift from HSP-2 to HSS-2 during MPF activation. The activation status of Cdc25C and presence of CyclinB2 in HSS-2 and HSP-2 were compared in four different extracts made at slightly different times in the cell cycle and designated i to iv as indicated at the top of the figure. From analysis of MPF activation in these extracts at 21°C (see text for details), we can deduce that extract i was made before activation, extracts ii and iii were made at the onset of activation, and extract iv was made during the activation of MPF, as stated at the bottom of the figure. The same region of a parallel gel stained with Coomassie blue is shown to allow comparison of protein loading. Approximate relative molecular weights in kilodaltons are shown on the left. For each extract i to iv paired samples of HSS-2 (left) and HSP-2 (right) were loaded as indicated below the lanes. Irrespective of the degree of MPF activation in these extracts, most of the faster migrating CyclinB2 isoform, representing pre-MPF (A) and inactive Cdc25C is pelleted into HSP-2.

used retrospectively as an indication of the extracts' cell cycle state at the time each was made. Extract i was made before activation had begun and reached peak activation at 40 min after transfer to 21°C. Extracts ii and iii were made at the onset of activation and reached peak activity after 10 min, and extract iv was made during the activation phase of MPF, such that it had already reached 90% of peak activation when it was fractionated.

In all four extracts the inactive form (lower band) of Cdc25C pelleted in the HSP-2 (right-hand lane of each pair) but increasingly activated (upper band) isoforms were found in the HSS-2 (left-hand lane of each pair). Similarly, inactive CyclinB2 was always sedimented in the HSP-2, whereas CyclinB2 was increasingly detectable in the HSS-2 as the cell cycle progressed and invariably migrated as its upper phosphorylated (active) form. The presence of the upper form of CyclinB2 in both HSP-2 and HSS-2 became more apparent in those extracts closest to full activation.

These comparisons thus revealed a clear correlation between the degree of MPF/Cdc25C activation in the eggs as they advance into M phase and the appearance of activated forms in the HSS-2 when fractionated. Furthermore, these comparisons suggest that MPF activation occurs first in association with the pelletable structures where active and inactive forms of CyclinB2 are detected together. Taken together, our analyses of MPF and Cdc25C compartmentalization in egg fractions indicate that MPF activation requires both soluble and structural components and is coupled to release from a pelletable fraction containing particulate material and AL membranes.

CyclinB2 Associates with Annulate Lamellae in Stage VI Oocytes

Studies from various cell types indicate that CyclinB-Cdc2 occupies distinct cellular compartments before mitosis. Because the only recognizable structures present in the HSP-2 were AL (see above), we wished to know whether the cofractionation of AL and pre-MPF in the HSP-2 reflected in vivo association of these elements. Unfortunately, the CyclinB antibodies available were not of high enough affinity to allow EM immunolocalization on pelleted material. Instead, we exploited the localization of characteristic AL in the vegetal subcortex of immature (stage VI) *Xenopus* oocytes (Terasaki *et al.*, 2001) to perform colocalization studies at the light microscope level. The size and opacity of the *Xenopus* egg is prohibitive for clear visualization of deep structures such as the nucleus; however, the first 10–20 μm below the cell surface where the AL lie is easily accessible to confocal microscopy in both fixed and live eggs. Immature oocytes are naturally arrested at prophase of meiosis and thus are at an equivalent cell cycle state to the activated eggs used in the extract fractionation experiments just described. We used CyclinB2 as a marker for the distribution of pre-MPF because it is the major B type cyclin present in stage VI oocytes (Kobayashi *et al.*, 1991) and is almost exclusively present as a complex with Cdc2 (Solomon *et al.*, 1990; Ookata *et al.*, 1992).

The distribution of AL, the ER protein GRP94, and CyclinB2 was first examined by a series of immunofluorescence experiments on fixed oocytes (Figure 6) and then by microinjection of GFP-CyclinB2 into stage VI oocytes followed by live imaging of the vegetal cortex (Figure 7). AL, which can be clearly detected by the anti-NUP antibody used for Western blot experiments, show up as islands of various shapes, but mostly form long and narrow "cigars" ranging from 10 to 30 μm in length and 3–5 μm in width and depth (Figures 6, A and D, and 7E; Terasaki *et al.*, 2001). Double labeling for NUP and Grp94 (Figure 6, A and B) confirmed that the NUP-stained islands were embedded within the ER network (Figure 6C), consistent with the position of AL as an integral part of the ER network (Bal *et al.*, 1968; Kessel, 1992; Terasaki *et al.*, 2001). Strikingly, double labeling with anti-CyclinB2 and anti-NUP (Figure 6, D and E) revealed accumulations of anti-CyclinB2 on the AL as well as in spots distributed throughout the cytoplasm (see Figure 6F for overlay). The extent of localization of CyclinB2 at annulate lamellae and the amount of CyclinB2 on the AL was variable between experiments. This variability may, in part, be due to slight differences in fixation/processing or to the low affinity of the anti-CyclinB2 antibody. Note that the incomplete overlap in the anti-Nup and anti-CyclinB2 staining pattern would be consistent with Cyclin association to AL through structures other than pore components.

Examination of the distribution of a *Xenopus* CyclinB2-GFP protein in live oocytes confirmed the CyclinB2–AL association. A GFP-CyclinB2 mRNA was microinjected into stage VI oocytes and imaged at regular intervals by confocal microscopy. GFP fluorescence was first observed as islands at the vegetal cortex 2 to 4 h after microinjection (Figure 7B), strongly resembling the pattern and dimensions of the cigars detected by NUP antibody in the same region (Figure 7E). This pattern of CyclinB2-GFP was observed in three separate experiments. A mRNA coding for nonconjugated GFP was injected for comparison (Figure 7, C and D). The strongest accumulation of GFP fluorescence was observed in a shallower more cortical layer than that observed with CyclinB2-GFP (compare Figure 7C with 7A). At deeper levels, equivalent to those at which the AL are situated, some fluorescence was visible as more diffuse islands (compare Figure 7D with 7B). A group of the subcortical structures decorated by the CyclinB2-GFP is shown at higher magnification in Figure 7F and can be seen to be equivalent to the AL stained with anti-NUP in Figures 6 and 7E. We thus conclude that CyclinB2 associates with AL in live oocytes.

The AL-like pattern of GFP-CyclinB2 was more striking and had a less spotty appearance than that obtained by immunofluorescence in fixed oocytes. This difference may reflect structural changes upon fixation and poor detection by the antibody in immunofluorescence experiments, the lower concentration of endogenous CyclinB2, and/or the progression through meiosis in CyclinB2-GFP–expressing oocytes. Nevertheless, the observed localization of CyclinB2 at AL by these two different approaches is a strong indication that some proportion of the CyclinB2-Cdc2 pool associates with AL in prophase oocytes and that the cofractionation of pre-MPF and AL observed in the HSP-2 made from prophase activated eggs reflects an in vivo association.

DISCUSSION

MPF activation in both oocytes and fertilized eggs of *Xenopus* has been shown to initiate locally within the animal hemisphere (Masui, 1972; Rankin and Kirschner, 1997; Pérez-Mongiovi *et al.*, 1998) and to be stimulated by subcel-
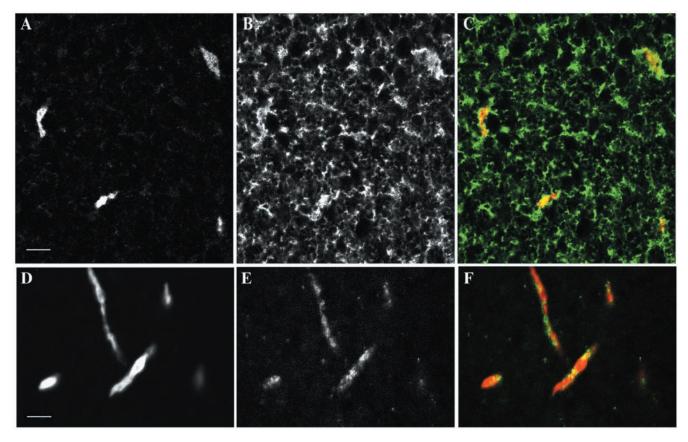
Figure 6. Detection of CyclinB2 at AL in stage VI oocytes. Confocal images of the vegetal cortex region of oocytes fixed and processed for double immunofluorescence by using anti-Nup and anti-GRP94 (A and B) and anti-Nup and anti-CyclinB2 (D and E). Superimposed images with anti-GRP94 or anti-CyclinB2 in green and anti-NUP in red are shown in C and F, respectively. Bars, 10 μm.

lular structures, including nuclei, centrosomes, and microtubule asters (Gautier, 1987; Li *et al.*, 1997; Iwashita *et al.*, 1998; Pérez-Mongiovi *et al.*, 2000), which may act to accumulate MPF and its regulators and/or other cellular components involved in activation in the perinuclear region. Despite these intriguing findings, relatively little attention has been paid to the subcellular association of MPF and its regulators in these cells. Immunofluorescence studies in *Xenopus* have been limited to a low-resolution study showing that CyclinB is concentrated in cortical and perinuclear rings in toad oocytes (Sakamoto *et al.*, 1998) as it is in *Drosophila* (Raff *et al.*, 1990). In this study, we revealed a cofractionation of characteristic AL together with pre-MPF from high-speed extracts of activated eggs. This finding prompted us to visualize CyclinB2 distribution in live and fixed oocytes, which confirmed that MPF associates with AL. We have thus provided evidence from complementary approaches that MPF associates with nuclear membranes at the onset of M phase. Note that we use the term "nuclear membranes" to include the excess nuclear envelope components that exist as cytoplasmic AL as well as the nuclear envelope proper. The association of pre-MPF with nuclear membranes provides an explanation for the influence of nuclei and centrosomes on MPF activation. It may also favor the nuclear/cytoplasmic shuttling of active MPF derived from a localized pool (Li

et al., 1997; Yang *et al.*, 1998; Hagting *et al.*, 1999). Furthermore, the specific targeting of CyclinB-Cdc2 to the nuclear envelope could facilitate the phosphorylation of nuclear envelope proteins, including nucleoporins, at mitosis necessary to promote nuclear envelope breakdown.

Annulate Lamellae, Nuclear Envelopes, and MPF Localization

AL are stacks of ER membranes containing a high density of nuclear pores, thought to form from excess nuclear membrane components, that have been described in a number of different cells, including oocytes from various species as well as rapidly proliferating cells. AL membranes are continuous with and embedded within the ER (this study, Figure 6, A—C; Kessel, 1992; Terasaki *et al.*, 2001), and it is not clear why they separate from the rest of the ER during fractionation, although the high concentration of nuclear pores is likely to significantly affect their density. AL accumulate in interphase *Xenopus* egg extracts (Dabauvalle *et al.*, 1991; Meier *et al.*, 1995) and disassemble in parallel with the nuclear envelope at mitosis/meiosis (Cordes *et al.*, 1996; Imreh and Hallberg, 2000; Terasaki *et al.*, 2001) and thus will be maximally accumulated at the time we made our extracts, favoring their identification in our study.
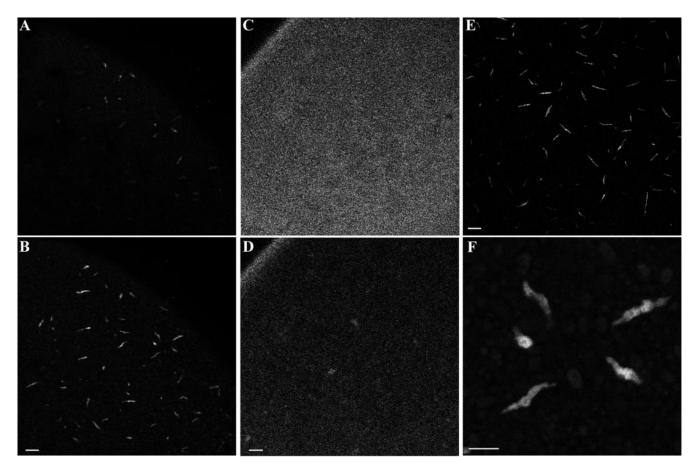
Figure 7. GFP-CyclinB2 localization to annulate lamellae in vivo. (A and B) An oocyte microinjected with CyclinB2-GFP mRNA and imaged by confocal microscopy 4 h later from the vegetal side. A shows the vegetal cortical layer, whereas B is at the level of the subcortical AL. (C and D) An oocyte microinjected with nonconjugated GFP mRNA. C shows the vegetal cortex, whereas D is a subcortical layer equivalent to that in B. Note in D the fluorescence in the oocyte cortical rim that is not apparent with the GFP-CyclinB2 in B. E a confocal image of AL labeled by immunofluorescence in a fixed oocyte by the anti-NUP antibody at the same magnification as A–D. Bars, 20 μm. F is a higher magnification image of islands labeled in B by the GFP-CyclinB2. Bar, 10 μm.

We were able to confirm that part of the MPF population in the undisturbed cell colocalizes with AL by two independent visualization methods applied to whole oocytes: immunofluorescence on fixed material and live imaging of GFP-CyclinB2. Cyclin B2-GFP expressed in immature oocytes localized to distinctive cigar-shaped structures located close to the vegetal surface with the characteristics defined for AL (Terasaki *et al.*, 2001), whereas an anti-cyclin B2 antibody decorated equivalent structures in fixed eggs, which we showed directly to be enriched in NUP proteins. It would be very hard to demonstrate association of MPF with the nuclear envelope in fertilized eggs because the tiny nucleus is hard to locate, whereas excess nuclear membrane components are dispersed throughout the volume of the egg. Because oocytes are naturally arrested in prophase, their cell cycle state is roughly equivalent to that of our extracts, made 60 min after activation ,and AL are concentrated in a visually accessible place. The microscopy data thus provide good evidence that the cofractionation of pre-MPF and AL from extracts reflects genuine in vivo association of these components at the onset of M phase; indeed, it

is remarkable that in spite of the fundamental differences that exist between cells in the meiotic and mitotic state, we find this identical association.

The association of pre-MPF with AL provides an explanation for the stimulation of MPF activation by nuclei and centrosomes and supports the suggestion that activation initiates at the nucleus/centrosome (Masui, 1972; Gautier, 1987; Shinagawa *et al.*, 1989; Iwao *et al.*, 1993; Li *et al.*, 1997; Rankin and Kirschner, 1997; Iwashita *et al.*, 1998; Pérez-Mongiovi *et al.*, 1998, 2000). For instance, centrosomal or perinuclear concentration of AL stacks has been observed in ascidians (Beckhelling, unpublished data; Roegiers *et al.*, 1999), insect oocytes (Rieder and Nowogrodzki, 1983), and sea urchin eggs (Kallenbach, 1982). These observations may help to explain the reported concentration of pre-MPF with other organelles in the perinuclear and/or pericentriolar region as well as to provide the basis for its association with nuclei in yeast (Alfa *et al.*, 1990; Audit *et al.*, 1996). Reexamination of published images shows association of CyclinB with the nuclear envelope at the onset of mitosis in *Drosophila* embryos (Wakefield *et al.*, 2000, supplementary material)

and subpopulations of Cyclin B1 and Cdc2 localized as a perinuclear ring during interphase in HeLa cells (Bailly *et al.*, 1992; Pockwinse *et al.*, 1997; Clute and Pines, 1999). These patterns may have been overlooked because of the strong localization of Cyclin B1 to centrosomes throughout interphase (Bailly *et al.*, 1992; Jackman *et al.*, 1995) or microtubules at mitosis (Jackman *et al.*, 1995) and that of Cyclin B2 at the Golgi in the pericentriolar area (Jackman *et al.*, 1995; reviewed in Beckhelling *et al.*, 2000; Ohi and Gould, 1999; Pines, 1999). Furthermore, recent detailed observations of Cyclin B distribution by immunofluorescence and Cyclin B-GFP expression in prophase starfish oocytes has revealed a clear association with the nuclear envelope (Terasaki, personal communication). Taken together, these observations support the suggestion that concentration of MPF in the perinuclear/pericentriolar area promotes MPF activation locally ahead of the rest of the cell (Beckhelling *et al.*, 2000).

The nature of the association of pre-MPF with nuclear membrane components and the mechanisms that may act to concentrate these components around the centrosome remain to be dissected. Nuclear pores are huge complexes containing up to 100 different polypeptides (Bagley *et al.*, 2000) that could provide potential links with pre-MPF itself or associated regulatory molecules. Pericentriolar distribution of pore proteins or other nuclear envelope components could be explained by their accumulation at microtubule minus ends via a documented association with cytoplasmic dynein (Reinsch and Karsenti, 1997; Beaudouin *et al.*, 2002; Salina *et al.*, 2002).

Pre-MPF Is Insoluble and MPF Solubilizes upon Activation

Our fractionation studies revealed a clear partitioning of pre-MPF and inactive Cdc25C into a pelletable fraction, whereas active MPF and active Cdc25C are found predominantly in the cytosol. Both active and inactive forms of MPF can be detected in the pellet depending upon the time of fractionation, suggesting that activation occurs in the pellet and then active forms shift to the supernatant. Other studies have also indicated that the localization of the MPF complex changes in parallel with its activation. A study in a *Xenopus* cell line showed that CyclinB1 shifts from a perinuclear site in prophase to a centrosomal and finally mitotic spindle location as the cycle progressed (Charrasse *et al.*, 2000). Analysis of MPF activity in fractionated human cells demonstrated that H1 kinase activates first in association with centrosomes, then in the cytoplasm, and last in the nucleus (De Souza *et al.*, 2000). Similarly, pre-MPF was found in a detergent-resistant fraction of human cells, whereas soluble MPF had high kinase activity, leading to the suggestion that active and inactive forms of MPF exist in equilibrium at the interface of structural/soluble cytoplasmic compartments (Bailly *et al.*, 1992).

In *Xenopus* egg extracts, Cyclin B1/Cdc2 has previously been shown to pellet after high-speed centrifugation (Leiss *et al.*, 1992). The conditions in that study would have pelleted all the material that we find distributed between HSP-1a, -1b, and HSP-2 in our protocol, thus making it difficult to identify which structures associated with these molecules. It is nevertheless clear that the major constituents of pre-MPF, CyclinB1/Cdc2 (Leiss *et al.*, 1992), and CyclinB2/Cdc2 (our study) as well as inactive Cdc25C, are insoluble. Furthermore, their release from associated structures leads to, or is concomitant with, activa-

tion to MPF. Simply adding CyclinB·90 to a cytosol where free Cdc2 exists, does not activate H1 kinase (Leiss *et al.*, 1992), suggesting that the presence of some other component of the pellet is critical for MPF activation.

Concluding Remarks

The results presented herein have uncovered the unexpected participation of nuclear membranes in activation of MPF. Associations for AL with a variety of molecular complexes have been reported; for instance, AL have been shown to colocalize with P granule material, associated with germ cell determination in *Caenorhabditis elegans* embryos (Pitt *et al.*, 2000). In another example, SUMO-1 protease SENP2 associates with NUP153 of the nuclear pore in humans (Hang and Dasso, 2002), as does a related protease with NUP42 in yeast (Takahashi *et al.*, 2000). The presence of AL at the vegetal cortex of the large *Xenopus* oocyte, and their reorganization at M phase that mirrors that of the nuclear envelope (Terasaki *et al.*, 2001), provides an excellent opportunity to further explore interaction of nuclear membranes with biologically important macromolecules in vivo. In particular a localization study of the various regulators of MPF such as Wee1, Myt1, the CDK inhibitor, Polo kinase, CyclinA-Cdc2, Pin1, CAK, and suc1 may further illuminate the basis of localized MPF regulation in the perinuclear region.

REFERENCES

Alfa, C.E., Ducommun, B., Beach, D., and Hyams, J.S. (1990). Distinct nuclear and spindle pole body population of cyclin-cdc2 in fission yeast. Nature *347*, 680–682.

Argon, Y., and Simen, B.B. (1999). GRP94, an ER chaperone with protein and peptide binding properties. Semin. Cell. Dev. Biol. *10*, 495–505.

Ashcroft, N.R., Srayko, M., Kosinski, M.E., Mains, P.E., and Golden, A. (1999). RNA-Mediated interference of a cdc25 homolog in *Caenorhabditis elegans* results in defects in the embryonic cortical membrane, meiosis, and mitosis. Dev. Biol. *206*, 15–32.

Audit, M., Barbier, M., Soyer-Gobillard, M.O., Albert, M., Géraud, M.L., Nicolas, G., and Lenaers, G. (1996). CyclinB (p56cdc13) localization in yeast *Schizosaccharomyces pombe*: an ultrastructural and immunocytochemical study. Biol. Cell *86*, 1–10.

Bagley, S., Goldberg, M.W., Cronshaw, J.M., Rutherford, S., and Allen, T.D. (2000). The nuclear pore complex. J. Cell Sci. *113*, 3885–3886.

Bailly, E., Doree, M., Nurse, P., and Bornens, M. (1989). p34cdc2 is located in both nucleus and cytoplasm; part is centrosomally associated at G2/M and enters vesicles at anaphase. EMBO J. *8*, 3985–3995.

Bailly, E., Pines, J., Hunter, T., and Bornens, M. (1992). Cytoplasmic accumulation of cyclin B1 in human cells: association with a detergent-resistant compartment and with the centrosome. J. Cell Sci. *101*, 529–545.

Bal, A.K., Jubinville, F., Cousineau, G.H., and Inoue, S. (1968). Origin and fate of annulate lamellae in Arbacia punctulata eggs. J. Ultrastruct. Res. *25*, 15–28.

Beaudouin, J., Gerlich, D., Daigle, N., Eils, R., and Ellenberg, J. (2002). Nuclear envelope breakdown proceeds by microtubule-induced tearing of the lamina. Cell *108*, 83–96.

Beckhelling, C., and Ford, C. (1998). Maturation promoting factor activation in early amphibian embryos: temporal and spatial control. Biol. Cell *90*, 467–476.

Beckhelling, C., Penny, C., Clyde, S., and Ford, C. (1999). Timing of calcium and protein synthesis requirements for the first mitotic cell cycle in fertilised *Xenopus* eggs. J. Cell Sci. *112*, 3975–3984.

Beckhelling, C., Pérez-Mongiovi, D., and Houliston, E. (2000). Localized MPF regulation in eggs. Biol. Cell *92*, .

Borgne, A., Ostvold, A.C., Flament, S., and Meijer, L. (1999). Intra-M phase-promoting factor phosphorylation of cyclin B at the prophase/metaphase transition. J. Biol. Chem. *274*, 11977–11986.

Brunati, A.M., Contri, A., Muenchbach, M., James, P., Marin, O., and Pinna, L.A. (2000). GRP94 (endoplasmin) co-purifies with and is phosphorylated by Golgi apparatus casein kinase. FEBS Lett. *471*, 151–155.

Charrasse, S., Lorca, T., Doree, M., and Larroque, C. (2000). The *Xenopus* XMAP215 and its human homologue TOG proteins interact with cyclin B1 to target p34cdc2 to microtubules during mitosis. Exp. Cell Res. *254*, 249–256.

Clute, P., and Pines, J. (1999). Temporal and spatial control of cyclin B1 destruction in metaphase. Nat. Cell Biol. *1*, 82–87.

Cordes, V.C., Reidenbach, S., and Franke, W.W. (1996). Cytoplasmic annulate lamellae in cultured cells: composition, distribution, and mitotic behavior. Cell Tissue Res. *284*, 177–191.

Cyert, M.S., and Kirschner, M.W. (1988). Regulation of MPF activity in vitro. Cell *53*, 185–195.

Dabauvalle, M.C., Loos, K., Merkert, H., and Scheer, U. (1991). Spontaneous assembly of pore complex-containing membranes ("annulate lamellae") in *Xenopus* egg extract in the absence of chromatin. J. Cell Biol. *112*, 1073–1082.

De Souza, C.P., Ellem, K.A., and Gabrielli, B.G. (2000). Centrosomal and cytoplasmic Cdc2/cyclin B1 activation precedes nuclear mitotic events. Exp. Cell Res. *257*, 11–21.

Detlaff, T.A., Nikitina, L.A., and Stoeva, O.G. (1964). The role of the germinal vesicle in oocyte maturation in anurans as revealed by the removal and transplantation of nuclei. J. Embryol. Exp. Morphol. *12*, 851–873.

Dumont, J.N. (1972). Oogenesis in *Xenopus laevis* (*Dandin*) 1. Stages of oocyte development in laboratory maintained animals. J. Morph. *136*, 153–180.

Edgar, B.A., Sprenger, F., Duronio, R.J., Leopold, P., and O'Farrell, P.H. (1994). Distinct molecular mechanism regulate cell cycle timing at successive stages of Drosophila embryogenesis. Genes Dev. *8*, 440–452.

Felix, M.A., Pines, J., Hunt, T., and Karsenti, E. (1989). A post-ribosomal supernatant from activated *Xenopus* eggs that displays post-transla-

tionally regulated oscillation of its cdc2+ mitotic kinase activity. EMBO J.EMBO J. *8*, 3059–3069.

Gautier, J. (1987). The role of the germinal vesicle for the appearance of maturation-promoting factor activity in the axolot oocyte. Dev. Biol. *123*, 483–486.

Gerhart, J.C., Wu, M., and Kirschner, M. (1984). Cell-cycle dynamics of an M-phase-specific cytoplasmic factor in *Xenopus laevis* oocytes and eggs. J. Cell Biol. *98*, 1247–1255.

Hagting, A., Jackman, M., Simpson, K., and Pines, J. (1999). Translocation of cyclin B1 to the nucleus at prophase requires a phosphorylation-dependent nuclear import signal. Curr. Biol. *9*, 680–689.

Hang, J., and Dasso, M. (2002). Association of the human SUMO-1 protease SENP2 with the nuclear pore. J. Biol. Chem. *277*, 19961–19966.

Hara, K., Tydeman, P., and Kirschner, M. (1980). A cytoplasmic clock with the same period as the division cycle in *Xenopus* eggs. Proc. Natl. Acad. Sci. USA *77*, 462–466.

Hartley, R.S., Rempel, R.E., and Maller, J.L. (1996). In vivo regulation of the early embryonic cell cycle in *Xenopus*. Dev. Biol. *173*, 408–419.

Heim, R., Cubitt, A.B., and Tsien, R.Y. (1995). Improved green fluorescence. Nature *373*, 663–664.

Imreh, G., and Hallberg, E. (2000). An integral membrane protein from the nuclear pore complex is also present in the annulate lamellae: implications for annulate lamella formation. Exp. Cell Res. *259*, 180–190.

Iwao, Y., and Elinson, R.P. (1990). Control of sperm nuclear behavior in physiologically polyspermic newt eggs: possible involvement of MPF. Dev. Biol. *142*, 301–312.

Iwao, Y., Sakamoto, N., Takahara, K., Yamashita, M., and Nagahama, Y. (1993). The egg nucleus regulates the behavior of sperm nuclei as well as cycling of MPF in physiologically polyspermic newt eggs. Dev. Biol. *160*, 15–27.

Iwashita, J., Hayano, Y., and Sagata, N. (1998). Essential role of germinal vesicle material in the meiotic cell cycle of *Xenopus* oocyte. Proc. Natl. Acad. Sci. USA *95*, 4392–4397.

Jackman, M., Firth, M., and Pines, J. (1995). Human cyclins B1 and B2 are localized to strikingly different structures: B1 to microtubules, B2 primarily to the Golgi apparatus. EMBO J. *14*, 1646–1654.

Kallenbach, R.J. (1982). 'De novo'centrioles originate at sites associated with annulate lamellae in sea urchin eggs. Biosci. Rep. *2*, 959–966.

Kessel, R.G. (1992). Annulate lamellae: a last frontier in cellular organelles. Int. Rev. Cytol. *133*, 43–120.

Kimelman, D., Kirschner, M., and Scherson, T. (1987). The events of midblastula transition in *Xenopus* are regulated by changes in the cell cycle. Cell *48*, 399–407.

Kobayashi, H., Minshull, J., Ford, C., Goldsteyn, R., Poon, R., and Hunt, T. (1991). On the synthesis and destruction of A and B-type cyclins during oogenesis and meiotic maturation in *Xenopus laevis*. J. Cell Biol. *114*, 755–765.

Laemmli, U.K. (1970). Cleavage of structural proteins during the assembly of the head of bacteriophage T4. Nature *227*, 680–685.

Leiss, D., Felix, M.A., and Karsenti, E. (1992). Association of cyclin-bound p34cdc2 with subcellular structures in *Xenopus* eggs. J. Cell Sci. *102*, 285–297.

Li, J., Meyer, A.N., and Donoghue, D.J. (1997). Nuclear localization of cyclin B1 mediates its biological activity and is regulated by phosphorylation. Proc. Natl. Acad. Sci. USA *94*, 502–507.

Lindsay, H.D., Whitaker, M.J., and Ford, C.C. (1995). Calcium requirements during mitotic cdc2 kinase activation and cyclin degradation in *Xenopus* egg extracts. J. Cell Sci. *108*, 3557–3568.

Liu, F., Stanton, J.J., Wu, Z., and Piwnica-Worms, H. (1997). The human Myt1 kinase preferentially phosphorylates Cdc2 on threonine 14 and localizes to the endoplasmic reticulum and Golgi complex. Mol. Cell. Biol. *17*, 571–583.

Masui, Y. (1972). Distribution of cytoplasmic activity inducing germinal vesicle breakdown in frog oocytes. J. Exp. Zool. *179*, 365–377.

Masui, Y., and Markert, C.L. (1971). Cytoplasmic control of nuclear behavior during meiotic maturation of frog oocytes. J. Exp. Zool. *117*, 129–145.

Meier, E., Miller, B.R., and Forbes, D.J. (1995). Nuclear pore complex assembly studied with a biochemical assay for annulate lamellae formation. J. Cell Biol. *129*, 1459–1472.

Moreno, S., and Nurse, P. (1990). Substrates for p34cdc2: in vivo veritas? Cell *61*, 549–551.

Morgan, D.O. (1997). Cyclin-dependent kinases: engines, clocks and microprocessors. Annu. Rev. Dev. Biol. *13*, 261–291.

Morgan, D.O. (1999). Regulation of the APC and the exit from mitosis. Nat. Cell Biol. *1*, E47–E53.

Murray, A., and Kirschner, M. (1989). Cyclin synthesis drives the early embryonic cell cycle. Nature *339*, 275–280.

Murray, A.W., Solomon, M.J., and Kirscner, M.W. (1989). The role of cyclin synthesis and degradation in the control of maturation promoting factor activity. Nature *339*, 280–286.

Newport, J., and Kirschner, M. (1984). Regulation of the cell cycle during early *Xenopus* development. Cell *37*, 731–742.

Nigg, E.A. (1995). Cyclin-dependent protein kinases: key regulators of the eukaryotic cell cycle. Bioessays *17*, 471–480.

Norbury, C., and Nurse, P. (1992). Animal cell cycles and their control. Annu. Rev. Biochem. *61*, 441–468.

Novak, B., and Tyson, J.J. (1993). Numerical analysis of a comprehensive model of M-phase control in *Xenopus* oocyte extracts and intact embryos. J. Cell Sci. *106*, 1153–1168.

Nurse, P. (1990). Universal control mechanism regulating onset of M-phase. Nature *344*, 503–508.

O'Farrell, P.H. (2001). Triggering the all-or-nothing switch into mitosis. Trends Cell Biol. *11*, 512–519.

Ohi, R., and Gould, K.L. (1999). Regulating the onset of mitosis. Curr. Opin. Cell Biol. *11*, 267–273.

Ookata, K., Hisanaga, S., Okano, T., Tachibana, K., and Kishimoto, T. (1992). Relocation and distinct subcellular localization of p34cdc2-cyclin B complex at meiosis reinitiation in starfish oocytes. EMBO J. *11*, 1763–1772.

Pante, N., Bastos, R., McMorrow, I., Burke, B., and Aebi, U. (1994). Interactions and three-dimensional localization of a group of nuclear pore complex proteins. J. Cell Biol. *126*, 603–617.

Pérez-Mongiovi, D., Beckhelling, C., Chang, P., Ford, C., and Houliston, E. (2000). Nuclei and microtubule asters stimulate maturation/M phase promoting factor (MPF) activation in *Xenopus* eggs and egg cytoplasmic extracts. J. Cell Biol. *150*, 963–974.

Pérez-Mongiovi, D., Chang, P., and Houliston, E. (1998). A propagated wave of MPF activation accompanies surface contraction waves at first mitosis in *Xenopus*. J. Cell Sci. *111*, 385–393.

Pines, J. (1999). Four-dimensional control of the cell cycle. Nat. Cell Biol. *1*, E73–E79.

Pitt, J.N., Schisa, J.A., and Priess, J.R. (2000). P granules in the germ cells of *Caenorhabditis elegans* adults are associated with clusters of nuclear pores and contain RNA. Dev. Biol. *219*, 315–333.

Pockwinse, S.M., Krockmalnic, G., Doxsey, S.J., Nickerson, J., Lian, J.B., van Wijnen, A.J., Stein, J.L., Stein, G.S., and Penman, S. (1997). Cell cycle independent interaction of CDC2 with the centrosome, which is associated with the nuclear matrix-intermediate filament scaffold. Proc. Natl. Acad. Sci. USA *94*, 3022–3027.

Raff, J.W., Whitfield, W.G., and Glover, D.M. (1990). Two distinct mechanisms localize cyclin B transcripts in syncytial *Drosophila* embryos. Development *110*, 1249–1261.

Rankin, S., and Kirschner, M.W. (1997). The surface contraction waves of *Xenopus* eggs reflect the metachronous cell-cycle state of the cytoplasm. Curr. Biol. *7*, 451–454.

Reinsch, S., and Karsenti, E. (1997). Movement of nuclei along microtubules in *Xenopus* egg extracts. Curr. Biol. *7*, 211–214.

Rieder, C.L., and Nowogrodzki, R. (1983). Intranuclear membranes and the formation of the first meiotic spindle in *Xenos peckii* (*Acroschismus wheeleri*) oocytes. J. Cell Biol. *97*, 1144–1155.

Roegiers, F., Djediat, C., Dumollard, R., Rouviere, C., and Sardet, C. (1999). Phases of cytoplasmic and cortical reorganizations of the ascidian zygote between fertilization and first division. Development *126*, 3101–3117.

Sakamoto, I., Takahara, K., Yamashita, M., and Iwao, Y. (1998). Changes in cyclin B during oocyte maturation and early embryonic cell cycle in the newt, *Cynops pyrrhogaster*: requirement of germinal vesicle for MPF activation. Dev. Biol. *195*, 60–69.

Salina, D., Bodoor, K., Eckley, D.M., Schroer, T.A., Rattner, J.B., and Burke, B. (2002). Cytoplasmic dynein as a facilitator of nuclear envelope breakdown. Cell *108*, 97–107.

Shinagawa, A. (1983). The interval of the cytoplasmic cycle observed in non-nucleate egg fragments in longer than that of the cleavage cycle in normal eggs of *Xenopus* laevis. J. Cell Sci. *64*, 147–162.

Shinagawa, A. (1992). Relative timing of stiffening with various combinations of nucleate and enucleated egg fragments of *Xenopus laevis*. Dev. Growth Differ. *34*, 419–425.

Shinagawa, A., Konno, S., Yoshimoto, Y., and Hiramoto, Y. (1989). Nuclear involvement in localization of the initiation site of surface contraction waves in *Xenopus* eggs. Dev. Growth Differ. *31*, 249–255.

Solomon, M.J., Glotzer, M., Lee, T.H., Philiphe, M., and Kirschner, M.W. (1990). Cyclin activation of p34cdc2. Cell *63*, 1013–1024.

Takahashi, Y., Mizoi, J., Toh-e, A., and Kikuchi, Y. (2000). Yeast Ulp1, an Smt3-specific protease, associates with nucleoporins. J. Biochem. *128*, 723–725.

Takizawa, C.G., and Morgan, D.O. (2000). Control of mitosis by changes in the subcellular location of cyclin-B1-Cdk1 and Cdc25C. Curr. Opin. Cell Biol. *12*, 658–665.

Terasaki, M., Runft, L.L., and Hand, A.R. (2001). Changes in organization of the endoplasmic reticulum during *Xenopus* oocyte maturation and activation. Mol. Biol. Cell *12*, 1103–1116.

Wakefield, J.G., Huang, J.Y., and Raff, J.W. (2000). Centrosomes have a role in regulating the destruction of cyclin B in early *Drosophila* embryos. Curr. Biol. *10*, 1367–1370.

Xu, X., Decker, W., Sampson, M.J., Craigen, W.J., and Colombini, M. (1999). Mouse VDAC isoforms expressed in yeast: channel properties and their roles in mitochondrial outer membrane permeability. J. Membr. Biol. *170*, 89–102.

Yang, J., Bardes, E.S.G., Moore, J.D., Brennan, J., Powers, M.A., and Kornbluth, S. (1998). Control of cyclin B1 localization through regulated binding of the nuclear export factor CRM1. Genes Dev. *12*, 2131–2143.

Zernicka-Goetz, M., Pines, J., Ryan, K., Siemering, K.R., Haseloff, J., Evans, M.J., and Gurdon, J.B. (1996). An indelible lineage marker for *Xenopus* using a mutated green fluorescent protein. Development *122*, 3719–3724.